Electronic Supplementary Material (ESI) for Energy & Environmental Science

Supporting information

Direct observation of charge separation on Au localized surface plasmon

Jacinto Sá, Giulia Tagliabue, Peter Friedli, Jakub Szlachetko, Mercedes H. Rittmann-Frank, Fabio G. Santomauro, Christopher J. Milne, and Hans Sigg

Experimental:

Materials and standard characterization

The high-resolution x-ray absorption spectroscopy (HR-XAS) measurements were performed on an array of Au nanoparticles (NPs) with a diameter of *ca.* 40nm (largely spaced > 100 nm) fabricated by block-copolymer lithography on 1 cm^2 Si chip. Fig.S1 shows a scanning electron microscope (SEM) image of the Si chip with Au NPs after preparation (1).

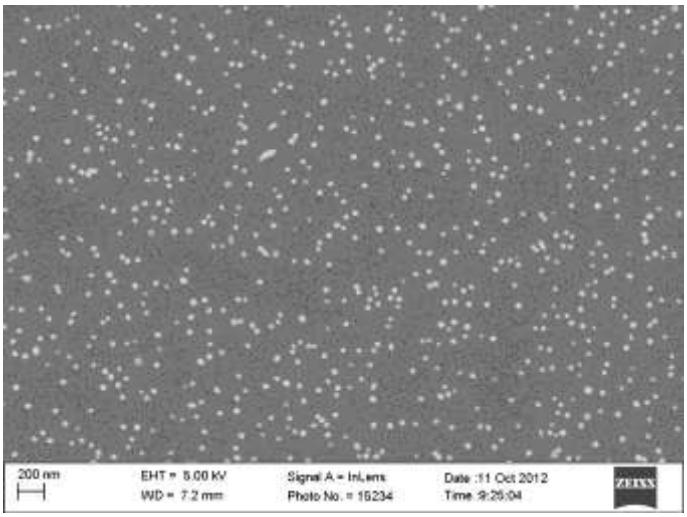

Fig. S1. SEM image Si chip coated with 40 nm Au NPs.

Transient mid-infrared (IR) measurements were performed on systems comprised of TiO_2 anatase powder coated with a sensitizer. Briefly, the TiO_2 NPs were prepared via the sol-gel method (2). The synthesis was carried out in a glove box under argon atmosphere. Titanium isopropoxide was dispersed in 10 mL 2-propanol. The resultant mixture was added drop wise under vigorous stirring to cold acidic water (2 °C, 250 mL H_2O, 18 M mixed with 80 mL glacial acetic acid, final pH 2). The sample was left under vigorous stirring in an ice bath for 12h. After which the sample was peptized at 80 °C for 2h until the liquid turns into a

transparent gel. The gel was autoclaved at 230 °C for 12 h. During this process the amorphous sample undergoes a phase transition leading to the formation of anatase NPs 20 nm (125 000 TiO_2 units) in size.

We used two types of sensitizers, namely:

- 30-40 nm Au NPs (Biocell) sparsely distributed and a loading 0.5 wt.% Au. A solution containing the NPs was added to a suspension of TiO_2 at room temperature. The sample was kept under vigorous stirring for 2h. The sample was dried overnight at 100 °C. The sample was used as prepared. Fig. S2 shows transmission electron microscopy (TEM) pictures of the sample. A suspension of Au-TiO_2 in ethanol was used to prepare TEM specimen.
- RuN719 dye was used as reference sensitizer. To achieve monolayer coverage of TiO_2 NPs nanoparticles at a concentration of 5 g/L we dissolve 170 mg of RuN719 in di-methyl formamide (DMF) (3). The anatase nanoparticles were mixed with the dye solution for half a day. To ensure that all dye is bonded to TiO_2, the suspension was left for several days in order to settle and then washed several times with DMF until the resultant DMF from the washing was clear. In order to avoid mid-IR signal saturation the sample was diluted tenfold with pure TiO_2.

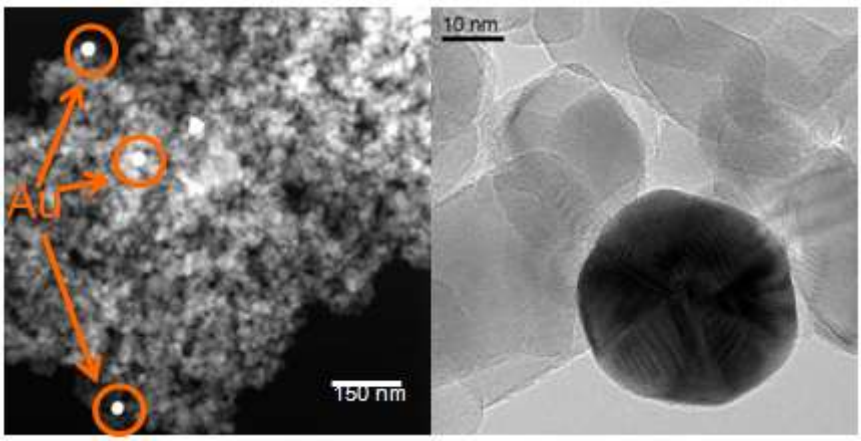

Fig. S2. TEM images of Au-TiO_2. A) Overview image depicting low-loading Au nanoparticle density; B) Image of a representative Au nanoparticle with roughly 30-40 nm diameter.

Representative UV-Vis spectra of the samples are depicted in Fig. S3. The samples were measured using a Perkin-Elmer Lambda 2000 spectrometer. The samples were measured as acidic water suspension concentration 0.5 mg/mL (sample/acid water), except the RuN719-TiO_2, which was measured with a dilution of 0.05mg/mL.

The UV-Vis spectrum of Au NPs reveal a peak centered at 544 nm ascribed to plasmonic resonance of gold. The peak decreases in intensity when the NPs are loaded onto TiO_2, which is associated with the dilution factor. The RuN719-TiO_2 reveals a characteristic absorption centered at around 525 nm. TiO_2 shows no absorption band in the region between 400-800 nm. The rising background measured for all samples containing TiO_2 are related to light scattering due to the 'milky' nature of the solution, especially for the more concentrated samples (TiO_2 and Au-TiO_2).

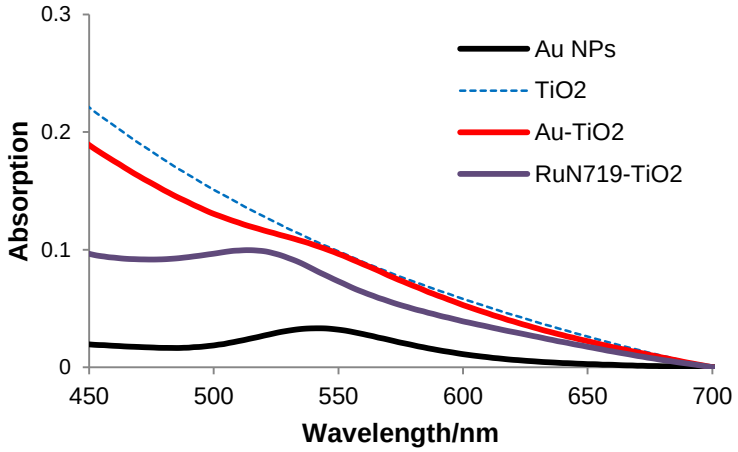

Fig. S3. UV-vis spectra of the mid-IR samples.

HR-XAS experiments

We performed HR-XAS, which is sensitive to metal density of states (DOS). Briefly, an array of Au NPs with a diameter of *ca.* 40nm (largely spaced > 100 nm) on 1 cm^2 Si chip was irradiated with incoming x-rays at a grazing incident angle *ca.* 1.5°. The x-rays photons were overlapped with continuous-wave laser (532 nm, 150 mW power) photons, also at a grazing incident angle *ca.* 2°.

The measurements were performed at the SuperXAS beamline of the Swiss Light Source (SLS) at the Paul Scherrer Institute, Switzerland. The X-ray beam delivered by the 2.9 Tesla super-cooled bending magnet was collimated by a spherically bent Rh mirror. The collimated X-rays were monochromatized by means of a double Si (111) crystal monochromator and focused by a toroidally bent Rh mirror. On the sample the photon flux was 7-8x10^{11} photons/sec with an energy resolution of $\Delta E/E \approx 1.4*10^{-4}$ and a spot size of 100x100 μm^2. For calibration a 4 μm thick Au foil was used.

The emitted x-rays were collected with a dispersive von Hamos-type spectrometer (4), which avoids component scanning during the acquisition. The grazing incidence experimental

geometry provides a line-like probe with a large number of irradiated particles thus enhancing the x-ray detection efficiency. Because the employed von Hamos geometry accepts a line-like source the grazing incident scheme does not affect the experimental resolution. To our knowledge, the application of grazing incidence with the von Hamos geometry is demonstrated here for the first time. Briefly, the x-rays emitted from the sample were diffracted by a Ge (660) crystal bent cylindrically to a radius of curvature of 25 cm. The crystal size was 10 cm and 5 cm in the focusing and dispersive axes, respectively. For the detection of the diffracted photons, a 1D-array, single photon counting, Mythen II was used. The spectrometer was operated in the vertical scattering geometry. Spectra were acquired around the Au L_{III}-edge located at 11919 eV.

FDMNES is a commonly used code to simulate X-ray absorption spectroscopy (XANES, XMCD) or resonant scattering (RXD) spectra collected at synchrotrons (5). Its *ab initio* approach reduces all the methodological parameters. FDMNES uses time dependent density functional theory (TD-DFT) for better description of excited states linked to the photon-matter interaction (6). The only change in the input parameter file performed was the electronic configuration of Au. It should be mentioned that the ionization threshold shift was corroborated by FEFF9.0 (7) calculations.

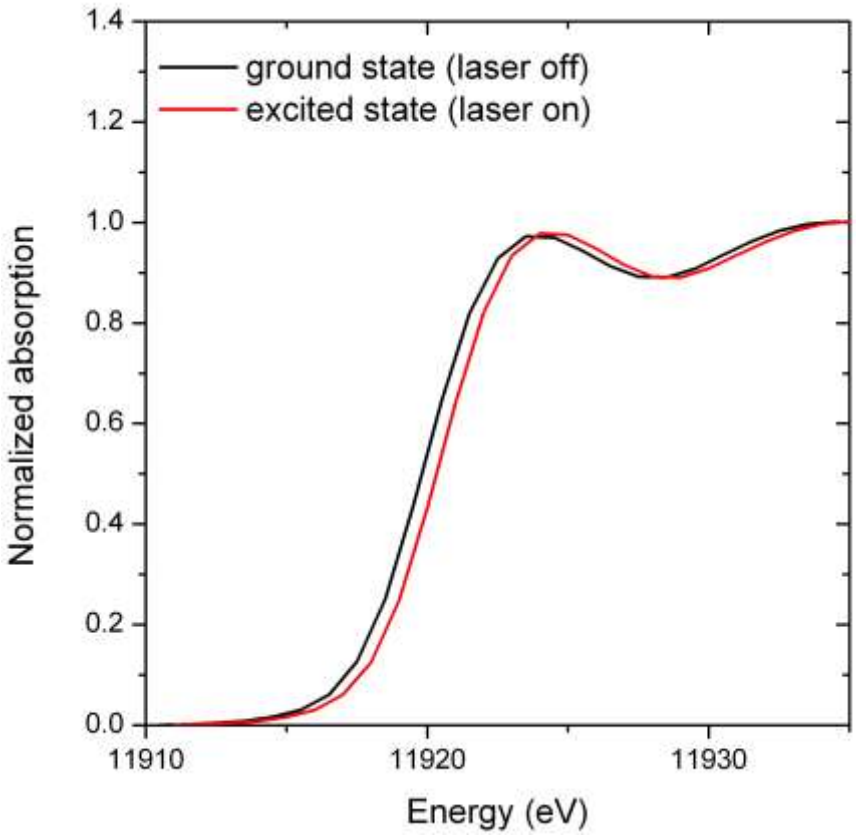

Fig. S4. HR-XAS spectra of excited and ground state Au NPs.

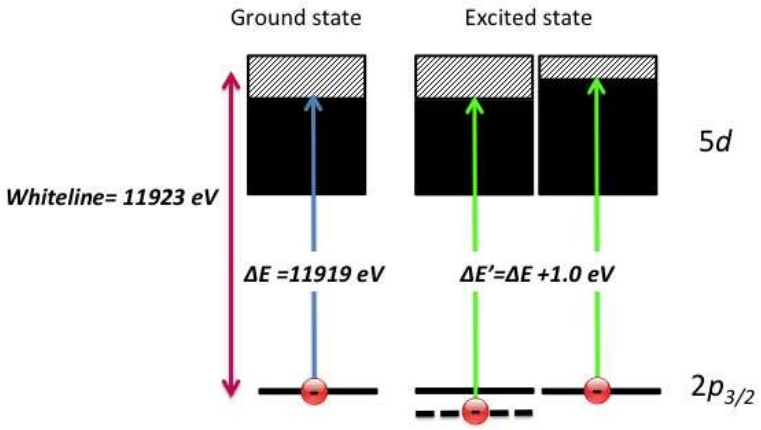

Fig. S5. Motifs responsible for the ionization threshold energy blue shift.

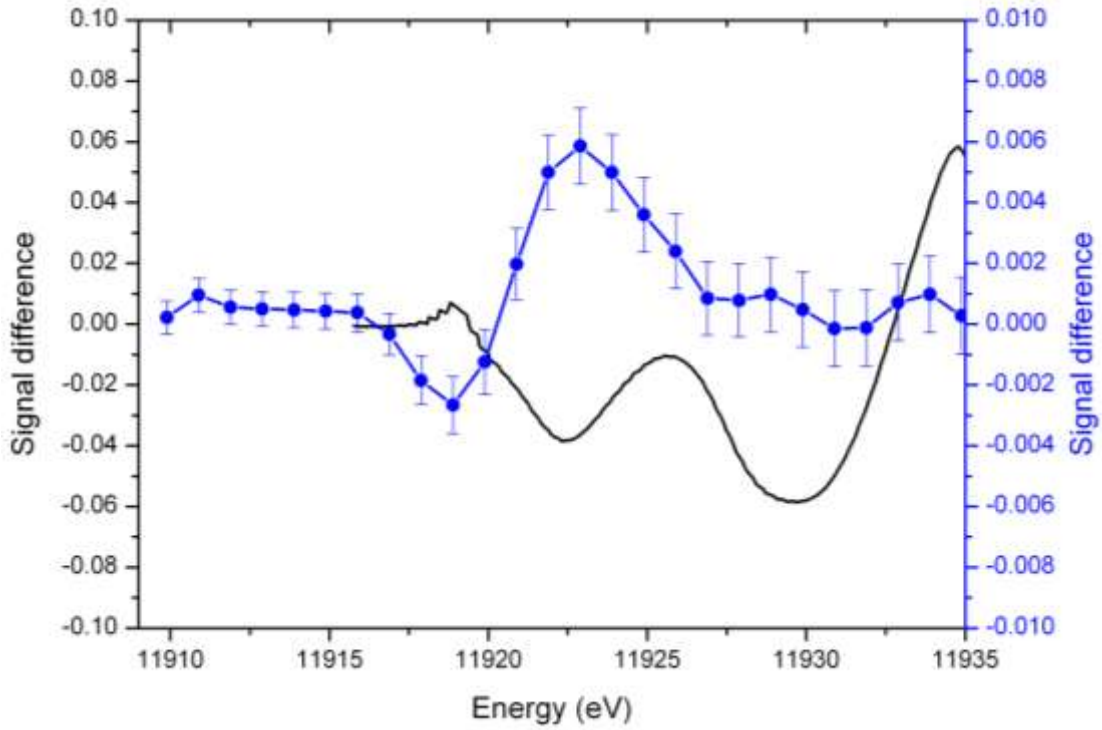

Fig. S6: Theoretical estimation of XAS spectral change due to thermal expansion. Blue measured signal and black the estimated signal changed due to 2% of Au lattice expansion, which equates to about 600 °C, according to Christensen (8).

Transient mid-IR experiments

We performed transient mid-IR absorption technique using the recently developed synchrotron based pump-probe setup with ~100 ps time resolution, as given by the synchrotron radiation bunch length, installed at the Infrared beamline of the SLS (9) (Fig. S7). Advantages of synchrotron-based experiments include large dynamic range and the sensitivity of the system combined with the large spectral bandwidth, which covers the entire mid-IR

range (approx. 625 to 10000 cm^{-1}). The multi-wavelength laser light system uses near-IR laser pulses generated by a Nd:YAG system and parametric down and up-conversion. A Phase-Lock Loop (PLL) control system locks the laser system to the SLS reference frequency of 500 MHz. The delay between the 80 ps pump pulse from the laser system and the relevant synchrotron radiation pulse, the so-called camshaft (4 times the charge of a standard bunch), is electronically tuned by a vector modulator (VM). This allows adding an arbitrary phase delay, and hence a time delay of up to 1 ms. The transmission of the camshaft pulses was measured with a fast Peltier-cooled mercury cadmium telluride (MCT) detector featuring a bandwidth of 800 MHz. The peak amplitude is digitized with a 14-bit resolution fast-sampling card, which records both pumped and unpumped transmission (arriving 1 μs in advance) instantaneously. Hence, this detection scheme is not susceptible to instabilities of the synchrotron source (manifested at the 1 to 3 kHz range) and slow drift phenomena, and it allows increasing the signal-to-noise ratio (S/N) of step-scan experiments significantly (typically by a factor of 100) on a time scale relevant to our experiments. The samples were excited with 33 mW of Nd:YAG pulsed monochromatic green (532nm) light. We used a resolution of 32 cm^{-1} to avoid contributions from RuN719 molecular vibrations. It should be mentioned that the signal is not associated with direct excitation of TiO_2 band gap because the pump does not have enough energy to overcome it and multi-photon absorption does not occur. To ensure good S/N, the presented spectra correspond to the average of data collected over a period of 24 h (2-3h per average spectrum).

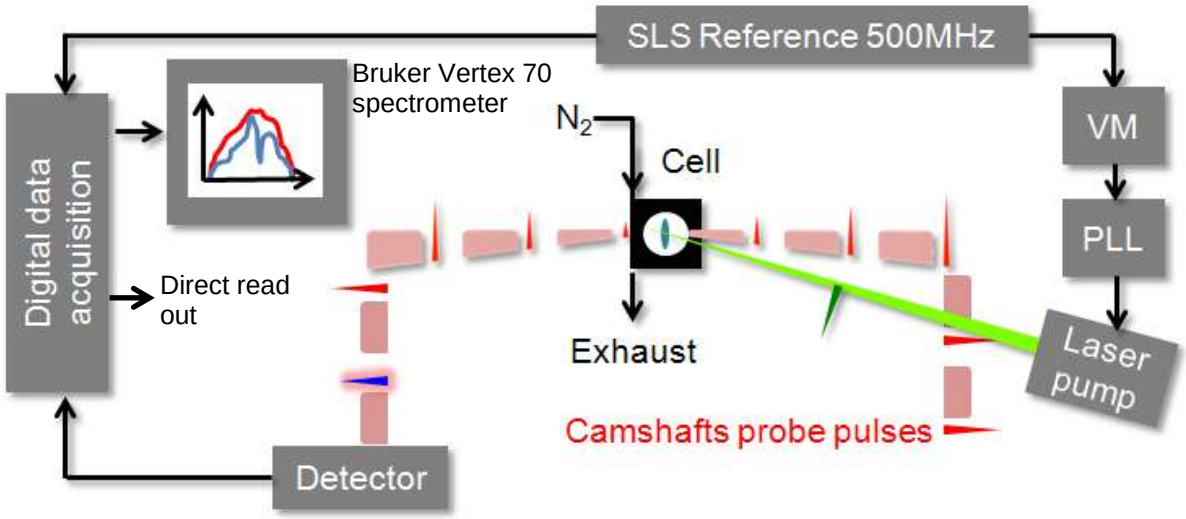

Fig. S7: Schematic representation of the SLS IR pump-probe setup. Both the pulsed laser at 532nm and the digital data acquisition were synchronized to the SLS reference frequency of 500MHz.

The cumulative changes are associated solely to the presence of electrons in TiO_2 conduction (changes of pump subtracted by unpumped spectra divided by umpumped). The changes obtained from the interferogram were found to be the same as the ones detected by integration of the signal difference directly from the digital data acquisition. Since direct read out decreases significantly the acquisition time, we used it to measure the signal difference at longer delay times (2- 80 ns). However it must be emphasized that this approach can only be used if one is evaluating a single event, which is the case.

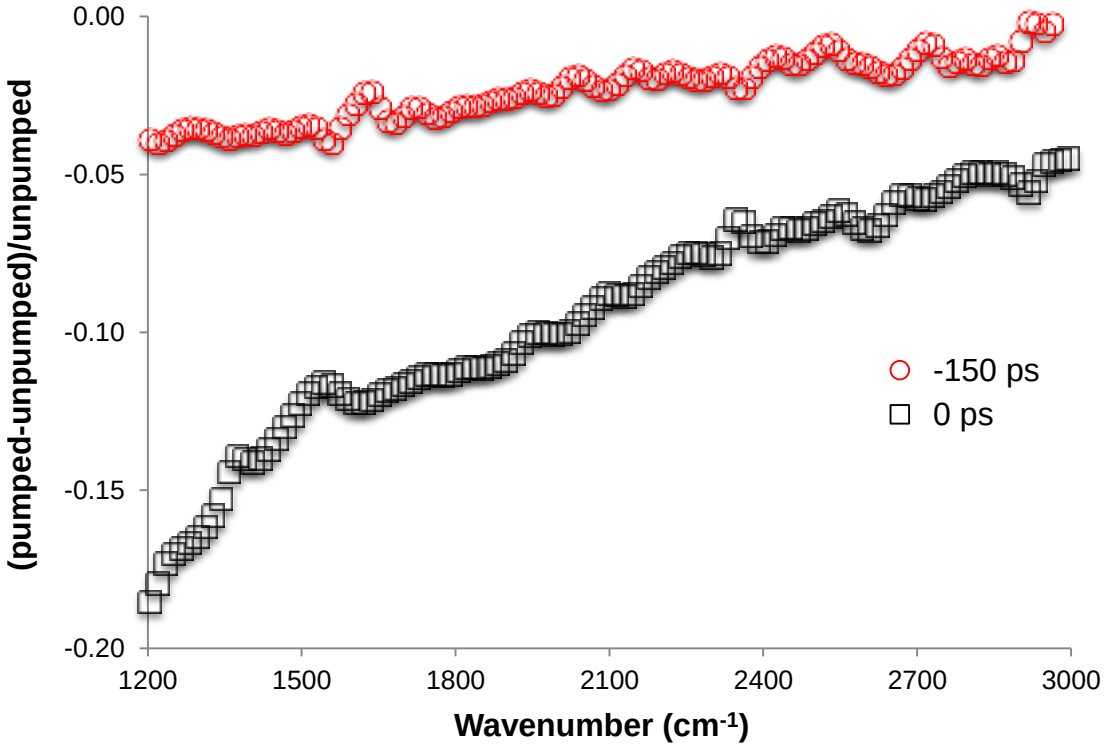

Figure S8. Time dependence of the mid-IR of TiO_2 coated with Ru-N719 dye irradiated at 532 nm with 100 ps pump pulses with energy of 33 μJ. Experimental resolution 32 cm^{-1}.

References

(1) a) T. Lohmueller, E. Bock, J. P. Spatz, Adv. Adv. Mater. 20, 2297 (2008); b) Roman Glass, Martin Möller, J. P. Spatz, Nanotechnol. 14, 1153 (2003).
(2) S. Mahshid, M. Askari, M. S. Ghamsari, *J. Mater. Proc. Technol.* **189**, 296 (2007)
(3) X. Zhang, G. Smolentsev, J. Guo, K. Attenkofer, C. Kurtz, G. Jennings, J. V. Lockard, A. B. Stickrath, L. X. Chen, *J. Phys. Chem. Lett.* **2**, 628 (2011).
(4) a) J. Szlachetko, M. Nachetgaal, E. de Boni, O. Safonova, J. Sá, G. Smolentsev, M. Szlachetko, J. A. van Bokhoven, J.-C. Dousse, J. Hoszowska, Y. Kayser, P. Jagodzinski, A. Bergamaschi, B. Schmid, C. David, A. Lücke, *Rev. Sci. Instrum.* **83**, 103105 (2012); b) J. Szlachetko, M. Nachtegaal, J. Sá, J.-C. Dousse, J. Hoszowska, E. Kleymenov, M. Janousch, O. V. Safonova, J. A. van Bokhoven, *Chem. Commun.* **48**, 10898 (2012).
(5) Y. Joly, *Phys. Rev. B* **63**, 125120 (2001).

(6) http://neel.cnrs.fr/spip.php?rubrique1007&lang=en
(7) a) A. L. Ankudinov, B. Ravel, J. J. Rehr, S. D. Conradson, *Phys. Rev B* **58**, 7565 (1998); b) J. J. Rehr, R. C. Albers, *Rev. Mod. Phys.* **72**, 621 (2000); c) A. L. Ankudinov, J. J. Rehr, J. Low, S. R. Bare, *Phys. Rev. Lett*. **86**, 1642 (2001).
(8) a) N.E. Christensen, *Phys. Rev. B* **20**, 3205 (1979); b) N.E. Christensen, B.O. Seraphin, *Phys. Rev. B* **4**, 3321 (1971).
(9) a) L. Carroll, P. Friedli, P. Lerch, J. Schneider, D. Treyer, S. Hunziker, S. Stutz, H. Sigg, *Rev. Sci. Instrum*. **82**, 063101(2011), b) J. Sá, P. Friedli, R. Geiger, P. Lerch, M. H. Rittmann-Frank, C. J. Milne, J. Szlachetko, F. G. Santomauro, J. A. van Bokhoven, M. Chergui, M. J. Rossi, Hans Sigg, *Analyst* DOI: 10.1039/c3an36595f.